the neuronal differentiation of either NTera2D1 or P19 cells (Fig. 3A). The mouse brain-specific miRNAs such as miR-125a, miR-125b, miR-136 and miR-9 appeared to be expressed, especially in differentiated P19 neurons (Fig. 3A), suggesting increase in the expression of these miRNAs during the morphological change of P19 cells after RA treatment. Other than the increased or decreased miRNAs during the neuronal differentiation, the miRNAs which appeared to significantly increase in their expression in the presence of RA were also detected in both the cells (Fig. 3B). In support of the observations, RT- (real time) PCR analysis with the TaqMan microRNA probes against the mouse miR-124a and -302c was carried out, and the results compatible with the data obtained from DNA chips were observed (Fig. 3C). Taken together, the observations suggest that regulation of miRNA expression in NTera2D1 and P19 cells was promptly changed by RA treatment. As a whole, the expression profiles of miRNAs during the neuronal differentiation of NTera2D1 and P19 cells appeared similar, suggesting comparable regulation of the expression of miRNAs in the course of neuronal differentiation. To further evaluate this, subsequent studies are necessary.

Expression profile of protein-coding genes related to neuronal differentiation

It is of interest and importance to see any relationships between the expression of miRNAs and protein-coding genes specific for neuronal development and/or differentiation during the differentiation of the cells examined here. For this purpose, we carried out RT-PCR analysis with total RNAs prepared from undifferentiated and differentiated cells. The investigated genes were as follows: *POU Domain, Class 5, Transcription Factor 1* (*POU5F1*); *Achaete-Scute Complex, Drosophila, homolog of, 1* (*ASCL1*), *Microtubule-Associated Protein 2* (*MAP2*); *Neurofilament Protein, Light Polypeptide* (*NEFL*); *Glial Fibrillary Acidic Protein* (*GFAP*); and *Glyceraldehyde-3-Phosphate Dehydrogenase* (*GAPDH*) as a control. Fig. 4 shows the results of RT-PCR analysis. The data of NTera2D1 and P19 cells

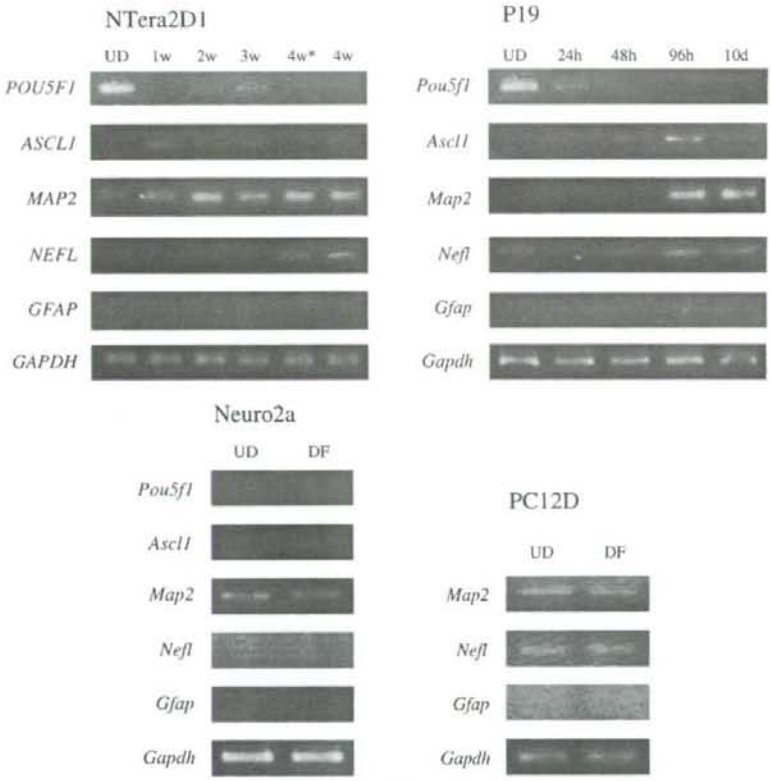

Fig. 4. Expression profiles of protein-coding genes related to neuronal differentiation. Total RNA was extracted from undifferentiated (UD) and differentiated (DF) cells. As for NTera2D1 and P19 cells, RNAs were prepared from the cells at various periods (indicated) after induction of differentiation: 1–4 weeks (1–4 w) in NTera2D1 cells and 24 h–10 days (24 h–10 d) in P19 cells. The RNAs were subjected to RT-PCR analysis to examine the expression of genes indicated. The expression of *Gapdh* was examined as a control. Asterisk indicates the NTera2D1 neurons grown on normal cultured plates instead of PDL-coated culture plates.

indicate: (i) the expression of *POU5F1* was detected in both of the undifferentiated cells, but rapidly reduced by RA treatment, (ii) an acute expression of *ASCL1* was detected after the RA treatment, (iii) *MAP2* and *NEFL*, which are specific to the neuron, appeared to increase in their expression after RA treatment and their potent expression was detected in the differentiated neurons, and (iv) little or no expression of *GFAP* was detected; meaning this could be due to the treatment of Ara-C during neuronal differentiation of the cells. Together with the expression profiles of the miR-302 cluster and miR-124a described above, it is likely that both the miRNAs and protein-coding genes were properly controlled during the differentiation of either NTera2D1 or P19 cells, and that the gene expression may be largely similar to authentic regulation of gene expression during neuronal development *in vivo*. Thus, we propose that expression of the miR-302 cluster and miR-124a could be molecular indicators for the degree of undifferentiation or differentiation in the course of neuronal differentiation in this kind of embryonic carcinoma or stem cells.

When N2a and PC12D cells were examined (Fig. 4), the expression of the neuron-specific *Map2* gene was detected in both the undifferentiated and differentiated cells. Interestingly, PC12D cells further expressed the *Nefl* gene at a state of either undifferentiation or differentiation. These observations suggest undifferentiated N2a and PC12D cells may be found more in neuronal differentiation than NTera2D1 and P19 cells. This indicates that they might stop differentiation before their morphologic changes, maintaining their undifferentiated state. Taken together, it is possible that a major change in the expression of genes, including miRNAs, would occur prior to morphologic changes with neurite outgrowth in the course of neuronal differentiation and/or development. To further evaluate this, more extensive studies must be conducted.

Acknowledgments

We thank Y. Nishiura and H. Oshima for their assistance. We also thank Dr. Y. Nagai for providing PC12D cells and for his helpful advice on cell culture. This work was supported in part by research grants from the Ministry of Health, Labour and Welfare of Japan and by Grants-in-Aid for Scientific Research from the Japan Society for the Promotion of Science.

Appendix A. Supplementary data

Supplementary data associated with this article can be found, in the online version, at doi:10.1016/j.bbrc.2007.07.189.

References

[1] Y. Lee, C. Ahn, J. Han, H. Choi, J. Kim, J. Yim, J. Lee, P. Provost, O. Radmark, S. Kim, V.N. Kim, The nuclear RNase III Drosha initiates microRNA processing, Nature 425 (2003) 415–419.

[2] A.M. Denli, B.B. Tops, R.H. Plasterk, R.F. Ketting, G.J. Hannon, Processing of primary microRNAs by the Microprocessor complex, Nature 432 (2004) 231–235.

[3] D.P. Bartel, MicroRNAs: genomics, biogenesis, mechanism, and function, Cell 116 (2004) 281–297.

[4] G. Hutvagner, P.D. Zamore, A microRNA in a multiple-turnover RNAi enzyme complex, Science 297 (2002) 2056–2060.

[5] A.M. Krichevsky, K.S. King, C.P. Donahue, K. Khrapko, K.S. Kosik, A microRNA array reveals extensive regulation of microRNAs during brain development, RNA 9 (2003) 1274–1281.

[6] J.G. Doench, C.P. Petersen, P.A. Sharp, siRNAs can function as miRNAs, Genes Dev. 17 (2003) 438–442.

[7] Y. Zeng, R. Yi, B.R. Cullen, MicroRNAs and small interfering RNAs can inhibit mRNA expression by similar mechanisms, Proc. Natl. Acad. Sci. USA 100 (2003) 9779–9784.

[8] C.G. Liu, G.A. Calin, B. Meloon, N. Gamliel, C. Sevignani, M. Ferracin, C.D. Dumitru, M. Shimizu, S. Zupo, M. Dono, H. Alder, F. Bullrich, M. Negrini, C.M. Croce, An oligonucleotide microchip for genome-wide microRNA profiling in human and mouse tissues, Proc. Natl. Acad. Sci. USA 101 (2004) 9740–9744.

[9] A.M. Cheng, M.W. Byrom, J. Shelton, L.P. Ford, Antisense inhibition of human miRNAs and indications for an involvement of miRNA in cell growth and apoptosis, Nucleic Acids Res. 33 (2005) 1290–1297.

[10] G.A. Calin, C.D. Dumitru, M. Shimizu, R. Bichi, S. Zupo, E. Noch, H. Aldler, S. Rattan, M. Keating, K. Rai, L. Rassenti, T. Kipps, M. Negrini, F. Bullrich, C.M. Croce, Frequent deletions and down-regulation of micro-RNA genes miR15 and miR16 at 13q14 in chronic lymphocytic leukemia, Proc. Natl. Acad. Sci. USA 99 (2002) 15524–15529.

[11] P.S. Eis, W. Tam, L. Sun, A. Chadburn, Z. Li, M.F. Gomez, E. Lund, J.E. Dahlberg, Accumulation of miR-155 and BIC RNA in human B cell lymphomas, Proc. Natl. Acad. Sci. USA 102 (2005) 3627–3632.

[12] L. He, J.M. Thomson, M.T. Hemann, E. Hernando-Monge, D. Mu, S. Goodson, S. Powers, C. Cordon-Cardo, S.W. Lowe, G.J. Hannon, S.M. Hammond, A microRNA polycistron as a potential human oncogene, Nature 435 (2005) 828–833.

[13] S.M. Johnson, H. Grosshans, J. Shingara, M. Byrom, R. Jarvis, A. Cheng, E. Labourier, K.L. Reinert, D. Brown, F.J. Slack, RAS is regulated by the let-7 microRNA family, Cell 120 (2005) 635–647.

[14] M. Lagos-Quintana, R. Rauhut, A. Yalcin, J. Meyer, W. Lendeckel, T. Tuschl, Identification of tissue-specific microRNAs from mouse, Curr. Biol. 12 (2002) 735–739.

[15] Y. Lee, M. Kim, J. Han, K.H. Yeom, S. Lee, S.H. Baek, V.N. Kim, MicroRNA genes are transcribed by RNA polymerase II, EMBO J. 23 (2004) 4051–4060.

[16] T. Babak, W. Zhang, Q. Morris, B.J. Blencowe, T.R. Hughes, Probing microRNAs with microarrays: tissue specificity and functional inference, RNA 10 (2004) 1813–1819.

[17] H.B. Houbaviy, M.F. Murray, P.A. Sharp, Embryonic stem cell-specific MicroRNAs, Dev. Cell 5 (2003) 351–358.

[18] E.A. Miska, E. Alvarez-Saavedra, M. Townsend, A. Yoshii, N. Sestan, P. Rakic, M. Constantine-Paton, H.R. Horvitz, Microarray analysis of microRNA expression in the developing mammalian brain, Genome Biol. 5 (2004) R68.

[19] H. Hohjoh, T. Fukushima, Expression profile analysis of microRNA (miRNA) in mouse central nervous system using a new miRNA detection system that examines hybridization signals at every step of washing, Gene 391 (2007) 39–44.

[20] T. Sakai, H. Hohjoh, Gene silencing analyses against amyloid precursor protein (APP) gene family by RNA interference, Cell Biol. Int. 30 (2006) 952–956.

[21] H. Hohjoh, M.F. Singer, Cytoplasmic ribonucleoprotein complexes containing human LINE-1 protein and RNA, EMBO J. 15 (1996) 630–639.

[22] J. Yu, F. Wang, G.H. Yang, F.L. Wang, Y.N. Ma, Z.W. Du, J.W. Zhang, Human microRNA clusters: genomic organization and expression profile in leukemia cell lines, Biochem. Biophys. Res. Commun. 349 (2006) 59–68.
[23] M.R. Suh, Y. Lee, J.Y. Kim, S.K. Kim, S.H. Moon, J.Y. Lee, K.Y. Cha, H.M. Chung, H.S. Yoon, S.Y. Moon, V.N. Kim, K.S. Kim, Human embryonic stem cells express a unique set of microRNAs, Dev. Biol. 270 (2004) 488–498.
[24] L.F. Sempere, S. Freemantle, I. Pitha-Rowe, E. Moss, E. Dmitrovsky, V. Ambros, Expression profiling of mammalian microRNAs uncovers a subset of brain-expressed microRNAs with possible roles in murine and human neuronal differentiation, Genome Biol. 5 (2004) R13.

Molecular Psychiatry (2007) 12, 519

www.nature.com/mp

IMAGE

The possible association between epigenetic aberration in DNA methylation in *RELN* and psychiatric disorders

Y Tamura[1], H Kunugi[1], J Ohashi[2] and H Hohjoh[1]

[1]*National Institute of Neuroscience, NCNP, Kodaira, Tokyo, Japan and* [2]*Department of Human Genetics, Graduate School of Medicine, The University of Tokyo, Bunkyo-ku, Tokyo, Japan*

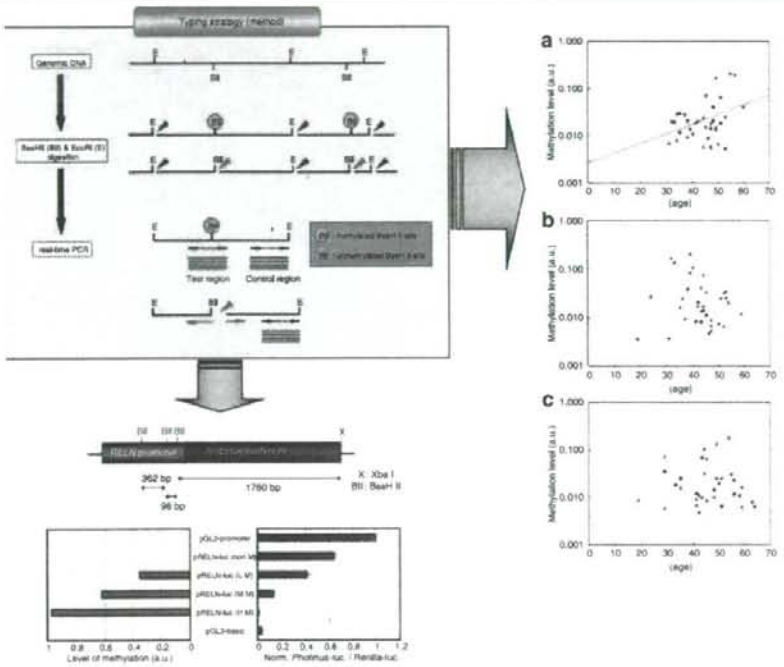

Molecular Psychiatry (2007) **12,** 519; doi:10.1038/sj.mp.4002014

Typing strategy (method) for determination of DNA methylation status: genomic DNA is digested with *Bss*HII, a methylation-sensitive restriction enzyme, and then subjected to real-time PCR such that a target region carrying a *Bss*HII site of interest can be amplified. In addition, regions adjacent to the target region, where no restriction enzyme sites are present, are also amplified and used as controls for normalization of the amplified target region. Using the method, the levels of DNA methylation in the human *REELIN* (*RELN*) gene in postmortem brain genomic DNA from schizophrenic, bipolar and healthy individuals were examined. The scatter graphs (the right panels) show that a statistically significant correlation between the levels of DNA methylation in *RELN* and age was detected in healthy individuals (**a**), no such correlations were seen in either schizophrenic or bipolar patients (**b** and **c**, respectively). The method can also be used for determination of DNA methylation status against the *RELN* reporter plasmids that are partially methylated *in vitro* (the downward arrow). The *in vitro* expression assay with the resultant reporter plasmids with various DNA methylation levels demonstrated a reverse correlation between the levels of DNA methylation and expression in *RLEN*. For more information on this topic, please refer to the article by Tamura *et al.* on pages 593–600.

Molecular Psychiatry (2007) 12, 593–600

www.nature.com/mp

ORIGINAL ARTICLE

Epigenetic aberration of the human *REELIN* gene in psychiatric disorders

Y Tamura[1], H Kunugi[1], J Ohashi[2] and H Hohjoh[1]

[1]*National Institute of Neuroscience, NCNP, Kodaira, Tokyo, Japan and* [2]*Department of Human Genetics, Graduate School of Medicine, The University of Tokyo, Bunkyo-ku, Tokyo, Japan*

Epigenetic genome modifications such as DNA methylation appear to be involved in various diseases. Here, we suggest that the levels of DNA methylation at the *BssH*II methylation-sensitive restriction enzyme sites in the human *REELIN* (*RELN*) gene in the forebrain vary among individuals. Interestingly, although a statistically significant correlation between the levels of DNA methylation in *RELN* and age was detected in healthy individuals, no such correlations were seen in either schizophrenic or bipolar patients. In addition, reverse correlations between DNA methylation levels and *RELN* expression were also detected in postmortem brain RNA and on *in vitro* assay. These data suggest the possibility that epigenetic aberration from the normal DNA methylation status of *RELN* may confer susceptibility to psychiatric disorders.
Molecular Psychiatry (2007) **12,** 593–600; doi:10.1038/sj.mp.4001965; published online 20 February 2007

Keywords: epigenetics; DNA methylation; REELIN; promoter activity; human postmortem forebrains

Introduction

DNA methylation is an epigenetic modification on the mammalian genome, and cytosine residues in CpG dinucleotides appear to be favorable targets for methylation, resulting in $C^{m}pG$. The process of DNA methylation and resultant $C^{m}pG$ appear to be involved in tissue-specific gene expression, chromatin modification and genomic imprinting, which play essential roles in development, cell proliferation and differentiation.[1,2] DNA methylation is also involved in various diseases, including cancer,[3] and may be associated with psychotic disorders such as schizophrenia.[4–8] To better understand the implications of DNA methylation in disease susceptibility, it is necessary to examine both the qualitative and quantitative status of DNA methylation within the genome.

In this study we developed a method by which relative levels of DNA methylation at methylation-sensitive restriction enzyme sites within the genome can be determined. The method depends on methylation-sensitive restriction enzymes and real-time polymerase chain reaction (real-time PCR). We investigated this method in order to determine any associations between DNA methylation and psychotic disorders by measuring the levels of DNA methylation in genomic DNA from schizophrenic, bipolar and healthy subjects using samples kindly provided by the Stanley Medical Research Institute.

The results presented here suggest that the levels of DNA methylation at methylation-sensitive restriction enzyme sites in the human *REELIN* (*RELN*) gene vary among individuals, and that a possible correlation between the levels of DNA methylation in *RELN* and age occurs in healthy individuals, but not in either schizophrenic or bipolar patients. The present study suggests the possible association between epigenetic aberration in DNA methylation in *RELN* and psychiatric disorders.

Materials and methods

DNA and RNA samples

All genomic DNA and RNA samples examined here were extracted from human postmortem forebrains and were kindly provided by the Stanley Medical Research Institute. Samples were blinded (coded) during our experiments (determination of DNA methylation and examination of expression levels), and after reporting all experimental data to the Institute, we obtained information regarding the diagnoses of the coded subjects, and then analyzed our typing data using subject information (Table 1).

Determination of relative DNA methylation levels

Genomic DNA (0.5 μg) was digested with *Eco*RI and *Bss*HII (methylation-sensitive restriction enzyme) at 37°C overnight, collected by ethanol precipitation, and dissolved in 50 μl of TE. Digested DNA (60 ng/

Correspondence: Dr H Hohjoh, National Institute of Neuroscience, NCNP, 4-1-1 Ogawahigashi, Kodaira, Tokyo 187-8502, Japan.
E-mail: hohjohh@ncnp.go.jp
Received 11 August 2006; revised 1 December 2006; accepted 19 December 2006; published online 20 February 2007

Table 1 Data of the subjects examined in this study

	Schizophrenia (n = *35*)	*Bipolar* (n = *35*)	*Control* (n = *35*)
Gender	26 males, nine females	17 males, 18 females	26 males, nine females
Age range (years at death)	19–59	19–64	31–60
Mean age (years)	43	46	45
Age at disease onset (years)			
⩽15	5	4	NA
16–20	14	9	NA
21–25	9	9	NA
26–30	3	4	NA
⩾31	4	9	NA
Lifetime alcohol use			
Little or no	10	4	18
Social	7	8	12
Moderate (past or present)	6	9	3
Heavy (past or present)	12	13	2
No information	0	1	0
Lifetime drug use			
Little or no	14	11	30
Social	4	4	4
Moderate (past or present)	6	9	1
Heavy (past or present)	9	11	0
No information	2	0	0
Suicide victims	7	15	0
Postmortem interval (hours)	9–80	12–84	9–58

Abbreviation: NA, not applicable.

test) was used as a template and was examined by means of real-time PCR using the following PCR primer sets:

For amplification of the control region of *RELN*;
RC-F1, 5′-GAACAGTCCGGCGAAGAGAG-3′
RC-R1, 5′-CAGAGCCTCATCTGTAGAGGATTT-3′
For the test region of *RELN*, we carried out real-time PCR with a *RELN* probe that we designed:
RC-F3, 5′-CGGCGTCTCCAAAACTGAATGA-3′
RC-R3, 5′-GTGGGGTTGCCCGCAATATGCAG-3′
RELN probe, 5′-(FAM)-CTAGCGCTGTTGCTGGGGGC GACGCTG-(TAMRA)-3′

Real-time PCR was carried out using the ABI PRISM 7000 or 7300 sequence detection system (Applied Biosystems, Foster City, CA, USA) with SYBR GREEN PCR Master Mix (for control region) or TaqMan Universal PCR Master Mix (for test region) according to the manufacturers' instructions and was repeated at least three times. Two individuals' samples were examined as controls for every PCR in order to normalize test data.

Cell culture
NTera2D1 cells were grown as described previously.[9] Cells ($\sim 7 \times 10^4/cm^2$) were treated with 10^{-5} M all-*trans*-retinoic acid (RA) (SIGMA-ALDRICH, St Louis, MO, USA) in Dulbecco's modified eagle medium (SIGMA-ALDRICH) supplemented with 10% fetal bovine serum (Invitrogen, Carlsbad, CA, USA), 100 U/ml penicillin (Invitrogen), and 100 μg/ml streptomycin (Invitrogen) for 3 weeks and reseeded ($\sim 5 \times 10^4/cm^2$), and further culture was carried out in the absence of RA.

Reverse transcription (RT)-(real-time) PCR
Total RNAs isolated from the same postmortem forebrain specimens were also provided by the Stanley Medical Research Institute, and each RNA sample (~ 0.5. μg) was examined by means of reverse transcription (RT) – real-time PCR (RT-PCR) with TaqMan Gene Expression Assays (Applied Biosystems) using TaqMan probes specific for *RELN* (assay ID: Hs00192449_m1) and *S18 rRNA* (assay ID: Hs99999901_s1) as a control. The assay RT-PCR) was carried out using the ABI PRISM 7000 or 7300 sequence detection system (Applied Biosystems) with TaqMan One Step RT-PCR Master Mix Reagents kit (Applied Biosystems) according to the manufacturer's instructions and was repeated at least three times.

Construction of reporter plasmid and partial methylation
In order to construct a reporter plasmid carrying a putative *RELN* promoter linked to the *Photinus luciferase* reporter gene, the *RELN* promoter region from positions −525 to +333 relative to the *RELN*

transcription start site was amplified by PCR with human genomic DNA and the following PCR primer set:

RELN-532F; 5′-GTTCTAGATCTTCCCAGGAAAAAC AGGGCACACTG-3′
RELN + misR; 5′-AATATCCATGGTGGCGAGCACCTC GCCCTGC-3′

The resultant PCR product was digested with *Bgl*II and *Nco*I and was subjected to ligation with pGL3-control treated with the same restriction enzymes. The resultant plasmid possessing the putative human *RELN* promoter was designated 'pRELN–Luc'.

Partial methylation was carried out as follows: ten micrograms of the pRELN–Luc plasmid was treated with 4 U of CpG methylase (M. Sss I) (New England BioLabs, Inc., Beverly, MA, USA) in the presence of 2×, 1× and 0.2× provided *S*-adenosyl methionine at 37°C for 6, 3 and 2 h, respectively. The treated plasmids were purified with a Wizard SV Gel and PCR clean-up system (Promega, Madison, WI, USA), and aliquots of the purified plasmids were subjected to digestion with *BamH*I and *BssH*II followed by real time PCR (1.25 ng each/test) for determination of DNA methylation levels. The PCR primer sets used were as follows:

For amplification of control region in the vector;
GL3-F1044, 5′-TTTGATATGTGGATTTCGAG-3′
GL3-R1194, 5′-ATCGTATTTGTCAATCAGAG-3′

For test region in the partially methylated *RELN*, the same PCR primers, RC-F3 and RC-R3, and the *RELN* probe described above were used. Real-time PCR and analyses of methylation levels were also carried out as described above.

Transfection

The day before transfection, NTera2D1 cells treated with RA for 3 weeks were trypsinized, diluted with fresh medium without RA and antibiotics, and seeded into 24-well culture plates (approximately 0.5×10^5 cells/well). Cotransfection of partially methylated pRELN–Luc plasmid with phRL–TK plasmid (Promega) as a control was carried out using Lipofectamine 2000 transfection reagent (Invitrogen) according to the manufacturer's instructions. Before cotransfection, the culture medium was replaced with 0.4 ml of OPTI-MEM I (Invitrogen), and to each well, 0.2 μg of

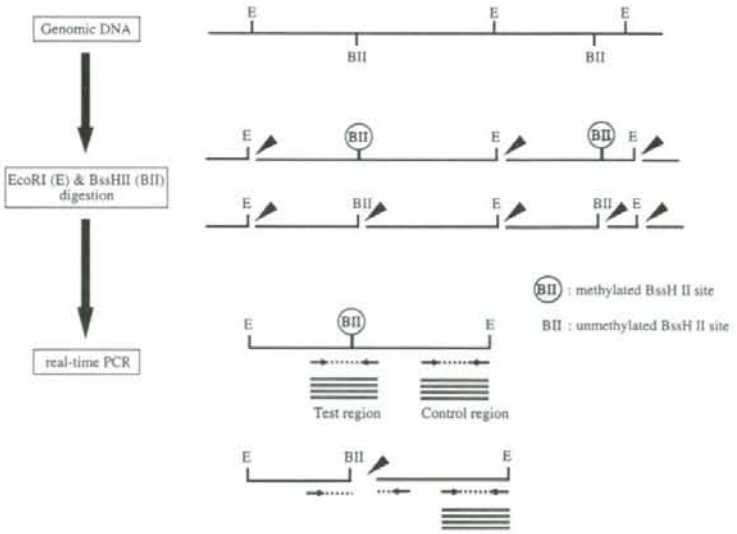

Figure 1 Outline of typing strategy for determination of DNA methylation status in the genome. Genomic DNA was digested with *EcoR*I and *BssH*II (methylation-sensitive restriction enzyme), and was subjected to real-time PCR such that a target region carrying *BssH*II site(s) of interest could be amplified. In addition, a region adjacent to the target region, where no *BssH*II sites were present, was also amplified and used as a control to normalize the amplified target region. When the *BssH*II site of interest in the target region was methylated, digestion of the site with the enzyme was inhibited, resulting in successful PCR amplification of the target region during real-time PCR. In contrast, when the *BssH*II site was not methylated, complete digestion of the site by the enzyme occurred, resulting in little or no PCR amplification. Accordingly, the level of DNA methylation at the *BssH*II site of interest in the target region is quantitatively reflected by the efficiency of real-time PCR amplification, and the observed amount of target region was subjected to normalization against that of the control region. A schematic representation is shown. *EcoR*I, unmethylated *BssH*II and methylated *BssH*II sites are indicated by 'E', 'BII', and 'BII', respectively. Arrow heads indicate restriction enzymes. PCR primers and amplified products are indicated by arrows and bars, respectively.

pRELN–Luc plasmid and 0.05 μg of phRL–TK plasmid were applied. Cells were incubated for 4 h at 37°C. After the 4-h incubation, 1 ml of the fresh culture medium without RA and antibiotics was added, and further incubation at 37°C was carried out. Forty-eight hours after transfection, cell lysate was prepared and expression levels of luciferase were examined by the Dual-Luciferase reporter assay system (Promega) according to the manufacturer's instructions.

Results and discussion

Typing strategy for determination of DNA methylation status

Figure 1 shows our typing strategy (method) for determination of DNA methylation status in the genome. Briefly, genomic DNA is digested with a methylation-sensitive restriction enzyme, and is then subjected to real-time PCR such that a target region carrying methylation-sensitive restriction enzyme site of interest can be amplified. In addition, regions adjacent to the target region, where no restriction enzyme sites are present, are also amplified and used as controls for normalization of the amplified target region. Compared with the method with bisulfite-modification of genomic DNA, the present method appears to have little or no bias from insufficient chemical modification of genomic DNA and biased PCR amplification with such a modified DNA in determination of methylation levels of target genes (or regions). Furthermore, this method, unlike a conventional Southern blot analysis with methylation-sensitive restriction enzymes, does not need a large amount of genomic DNA. Although the present system for determination of methylation levels appears to have the benefits that are not in conventional methods, the system profoundly depends upon methylation-sensitive restriction enzymes, by which investigation is usually restricted to the restriction enzyme sites; accordingly, this may be a major drawback of this method.

By using the method we investigated the levels of DNA methylation in genomic DNA from schizophrenic, bipolar and healthy subjects to determine any associations between DNA methylation and psychotic disorders. The genomic DNA examined in this study was extracted from human postmortem forebrains of schizophrenic, bipolar and healthy individuals (35 samples each) (Table 1), and was kindly provided by the Stanley Medical Research Institute.

DNA methylation status in RELN

We examined the human *REELIN* (*RELN*) gene, as its putative promoter region (including exon 1) includes a GC-rich sequence containing several methylation-sensitive restriction enzyme sites,[5] and because possible associations between this gene and psychotic disorders have been reported.[10–14] The methylation status at the *BssH*II sites (GCGCGC) in the promoter region was investigated using the above-described

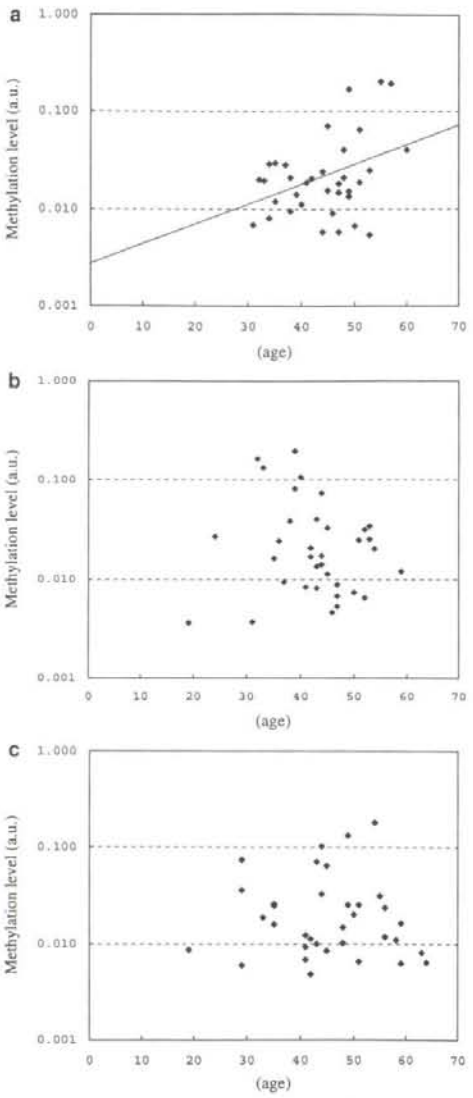

Figure 2 Scatter graphs of DNA methylation levels in *RELN* and age. All genomic DNA samples (35 samples each from healthy (**a**), schizophrenic (**b**) and bipolar (**c**) individuals) extracted from human postmortem forebrains were kindly provided by the Stanley Medical Research Institute. Relative levels of DNA methylation at *BssH*II sites in *RELN* were examined as described in Figure 1. Data regarding the levels of the DNA methylation are averages of three independent examinations and are given in arbitrary methylation units (a.u.). Tests for equal variance were carried out to determine whether there were any correlations between DNA methylation levels and aging.

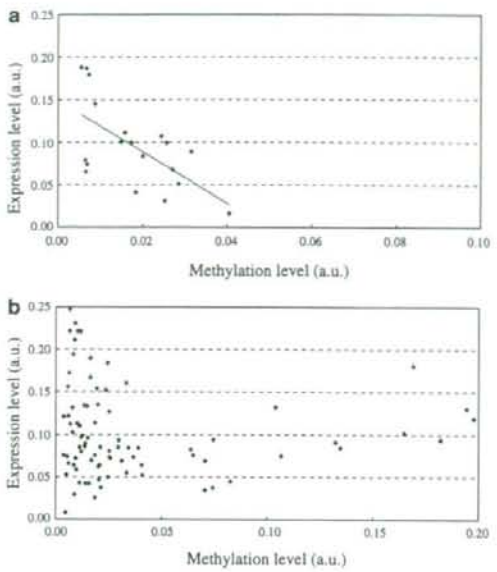

Figure 3 Relationship between DNA methylation levels and expression of *RELN*. Levels of expression of *RELN* and *18S rRNA* (control) among RNA samples extracted from the same postmortem forebrains as described in Figure 2 were examined by means of RT-PCR with TaqMan Gene Expression Assays (Applied Biosystems). Levels of expression of *RELN* were normalized against those of the control (18S rRNA). Data for DNA methylation and RNA expression are averages of three independent examinations and are given in arbitrary (methylation or expression) units (a.u.). Data for samples prepared within 18 h of death or beyond 18 h after death are shown in **a** and **b**, respectively. Tests for equal variance were performed to determine whether there were any correlations between the levels of DNA methylation and expression.

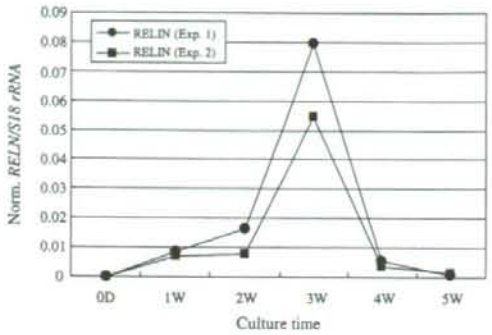

Figure 4 Expression profiles of *RELN* during neuronal differentiation of NTera2D1 cells. To investigate the endogenous expression of *RELN* during neuronal differentiation of NTera2D1 cells, expression profile analysis was carried out. Cells were treated with 10^{-5} M all-RA for 3 weeks and reseeded ($\sim 5 \times 10^4/cm^2$), and further culture was carried out in the absence of RA. Total RNA was extracted from cells before RA treatment (0 day: 0 D) and cells at the indicated time point after RA treatment (1 week ~ 5 weeks: 1 W ~ 5 W). Extracted RNAs were subjected to RT-PCR with TaqMan Gene Expression Assay as in Figure 3. Levels of *RELN* expression were normalized against those of *S18 rRNA*. Expression profile analysis was repeated twice independently (Exp.1 and Exp. 2). The results indicate that the expression of endogenous *RELN* is induced by RA treatment and that *RELN* expression peaks at around 3 weeks after RA treatment. Accordingly, we decided to use NTera2D1 cells treated with RA for 3 weeks host cells in the transient expression assay using partially methylated pRELN–Luc plasmids (Figure 5).

method. The results indicated that the relative levels of the DNA methylation varied among the schizophrenic, bipolar and healthy individuals. Because differences in the average levels of DNA methylation among the three groups did not reach statistical significance, further analyses stratified by age, gender, age at disease onset, life time alcohol and drug use and suicide status (Table 1) were carried out In this series of analyses, we identified an intriguing association; when DNA methylation levels and subject age were plotted in scatter graphs (Figure 2), a correlation between DNA methylation and age was seen in healthy individuals ($r = 0.436$, $P < 0.01$). It should be noted that no such correlation was seen in either schizophrenic or bipolar patients. In addition, it was observed that several patients under the age of 50 had higher levels of DNA methylation >0.03 (a.u.) at the level of DNA methylation shown in Figure 2: nine schizophrenia (25.7%) and seven bipolar (20.0%) cases met these criteria, but only three healthy individuals (8.6%) met these criteria. The difference in percentages between healthy individuals and either schizophrenic or bipolar patients, however, did not reach statistical significance owing to the small number of samples examined in this study. As for the other stratification analyses, we could not see their significant associations with the DNA methylation status in *RELN*.

Grayson *et al.* showed significant association of methylated cytosine at positions −139(CpApG) and −134(CpTpG) in *RELN* with schizophrenia by means of bisulfite-modification of genomic DNA followed by PCR amplification and sequence determination.[4] Our present study focused on the *BssH*II sites at positions +131, +227 and +229 in *RELN*. Therefore, different results between the previous and present studies may be attributable to the different positions examined.

Reverse correlation between the levels of DNA methylation and expression of the RELN *gene*

A previous study with completely methylated *RELN* promoter by CpG methylase (M.Sss I) suggested that DNA methylation of the *RELN* promoter *in vitro* decreased its promoter activity;[5] but correlations between DNA methylation levels in *RELN* and *RELN*

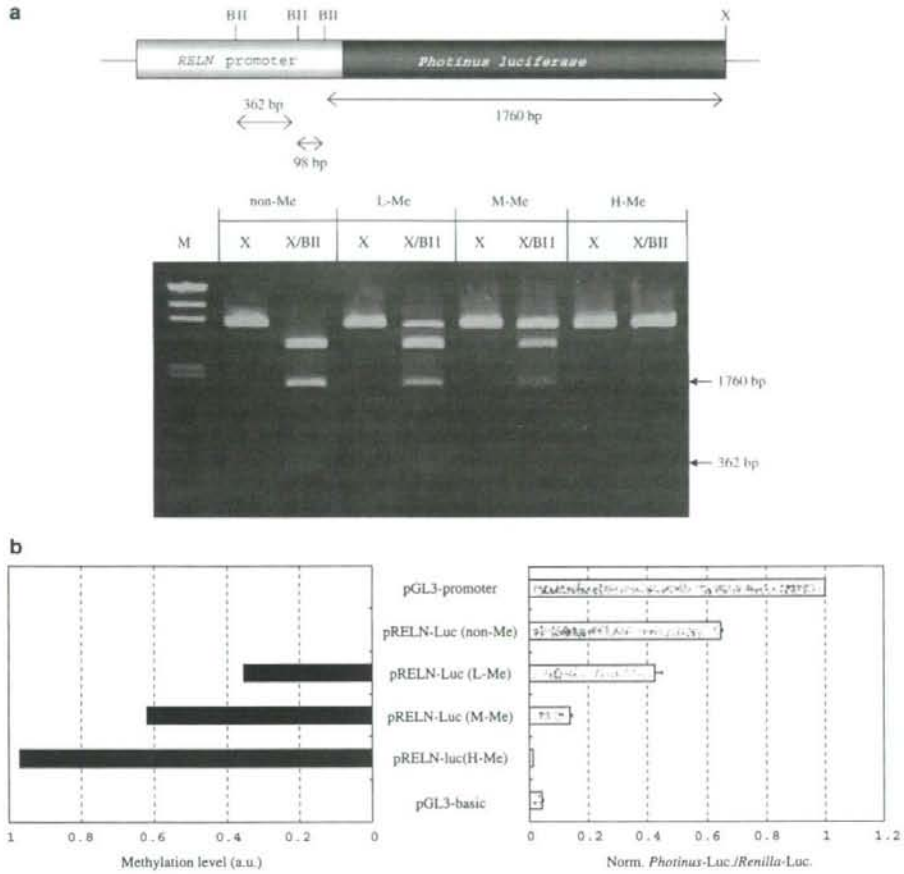

Figure 5 Reverse correlation between DNA methylation levels and transcriptional expression of *RELN*. (**a**) Digestion profiles of partially methylated plasmids with restriction enzymes. The pRELN–Luc plasmid carrying *Photinus luciferase* driven by the human *RELN* promoter was partially methylated using a CpG methylase (M. Sss I), after which the levels of DNA methylation were determined as in Figure 1. The resultant plasmids with various levels of DNA methylation, high (H-Me)-, moderate (M-Me)- and low (L-Me)-level methylated pRELN–Luc, were further confirmed by restriction enzyme digestion with *BssH* II (BII) and *Xba* I (X) followed by agarose gel electrophoresis. A schematic restriction enzyme map of pRELN–Luc is shown. Non-methylated plasmids and size markers (*Hind*III-cut λ DNA) are indicated by 'non-Me' and 'M', respectively. Note that the data also indicate that our typing method properly worked. (**b**) Reverse correlation between the levels of DNA methylation and expression of *RELN*. pRELN–Luc plasmids with various levels of DNA methylation were subjected to transfection together with phRL–TK encoding *Renilla luciferase* (control) into human teratocarcimona NTera2D1 cells treated with RA for 3 weeks, and in which endogenous *RELN* was being expressed (Figure 4). In addition, unmethylated SV40 promoter (in pGL3-Promoter) and no promoter (in pGL3-Basic) were also examined as positive and negative controls, respectively. Forty-eight hours after transfection, luciferase activities were examined. Test (*Photinus*) luciferase activity normalized against control (*Renilla*) luciferase activity and is given in arbitrary units (a.u.). Levels of DNA methylation are indicated as in Figure 2 and are given in arbitrary methylation units (a.u.).

expression remained unanswered. It is of interest and importance to determine whether there is any association between DNA methylation levels and expression in *RELN*. Total RNAs isolated from the same postmortem forebrains were also provided by the Stanley Medical Research Institute, and the expression levels of *RELN* and *18S rRNA* (control) were examined by means of RT-PCR. In the samples prepared within 18 h of death (eight schizophrenia and four bipolar cases, and seven healthy controls), a reverse correlation between DNA methylation and *RELN* expression was detected ($r=-0.63$, $P<0.01$), but no such correlation was seen in the samples prepared beyond 18 h after death (Figure 3). These

observations suggest that the level of DNA methylation in *RELN* likely influences its expression; and the observations also suggest the possibility that the postmortem DNA and/or RNA might undergo substantial degradation within 18 h of death. To address the possibility, more extensive studies must be carried out.

To further evaluate the correlation between DNA methylation levels and expression in *RELN*, we constructed a reporter plasmid carrying the *RELN* promoter region linked to the *Photinus luciferase* gene. The reporter plasmid was subjected to partial methylation with CpG methylase (M.Sss I), after which the level of DNA methylation was determined using the above-described method. The resultant reporter plasmids with various levels of DNA methylation (Figure 5a) and phRL–TK carrying *Renilla luciferase* (control) were cotransfected into NTera2D1 cells where endogenous *RELN* was expressed (Figure 4), that is, in which transacting (transcription) factors necessary for the proper *RELN* expression could occur. After incubation, luciferase expression levels in the transfected cells were examined. As shown in Figure 5b, *Photinus luciferase* expression decreased with increased levels of DNA methylation in the *RELN* promoter; thus, the results indicate a reverse correlation between the levels of DNA methylation and expression of the *RELN* gene. Together with the results shown in Figure 3a, the data strongly suggest that the level of DNA methylation in *RELN* is significantly associated with its expression. The previous study using the *RELN* promoters which were completely methylated *in vitro* with various bacterial methylases suggested that DNA methylation participated in downregulation of *RELN* expression.[5] Therefore, it is most likely that DNA methylation in *RELN* is a key element functioning in regulation of the expression of *RELN*.

Our present data appear to be compatible with those of the previous studies using bisulfite-modification of genomic DNA,[4,6] both suggesting the aberrant DNA methylation status of *RELN* in psychiatric disorders. In addition, recent studies also indicated that the mouse *DNA methyltransferase 1* (*Dnmt1*) gene knockdown was accompanied by increased expression of *Reln*[15] and that protracted administration of L-methionine, a precursor of the methyl donor *S*-adenosyl-methionine in Dnmt1 catalytic activity, into mice led to decreased *Reln* expression,[7] suggesting possible inhibitions of the expression of *Reln* involving DNA methylation *in vivo*. Altogether, it is conceivable that *RELN* may undergo various levels of epigenetic modifications of DNA methylation, and that aberrant DNA methylation status in *RELN* leading to aberrant expression may confer susceptibility to psychiatric disorders.

Genetic and epigenetic factors conferring susceptibility to psychiatric disorders

The human *RELN* gene is mapped to chromosome 7q22, where few associations with human genetic diseases, except for a possible association with Finnish schizophrenia,[16] have been reported, whereas significant reductions in *RELN* transcripts and polypeptides in the brains of patients with psychiatric disorders have been repeatedly observed.[10–14] The present study indicates the possible association between epigenetic aberration in DNA methylation in *RELN* and psychiatric disorders; such aberration is probably undetectable using conventional genetic analyses. It is conceivable that even though genes were negative for associations with diseases on conventional genetic analysis, genes such as *RELN* may be involved in disease susceptibility through aberrant epigenetic modifications. Therefore, to identify the culprits conferring susceptibility to diseases, extensive studies focusing on both genetic factors and epigenetic factors are required.

Acknowledgments

We thank Drs Michael B Knable, E Fuller Torrey, Maree J Webster, and Robert H Yolken in the Stanley Medical Research Institute for kindly providing genomic DNA and RNA samples. We also thank H Kimura and K Kaneko for their encouragement. This work was supported in part by research grants from the Ministry of Health, Labor, Welfare in Japan, and by a Grant-in-Aid from the Japan Society for the Promotion of Science.

References

1 Bird A. DNA methylation patterns and epigenetic memory. *Genes Dev* 2002; **16**: 6–21.
2 Jaenisch R, Bird A. Epigenetic regulation of gene expression: how the genome integrates intrinsic and environmental signals. *Nat Genet* 2003; **33**(Suppl): 245–254.
3 Robertson KD. DNA methylation and human disease. *Nat Rev Genet* 2005; **6**: 597–610.
4 Grayson DR, Jia X, Chen Y, Sharma RP, Mitchell CP, Guidotti A *et al*. Reelin promoter hypermethylation in schizophrenia. *Proc Natl Acad Sci USA* 2005; **102**: 9341–9346.
5 Chen Y, Sharma RP, Costa RH, Costa E, Grayson DR. On the epigenetic regulation of the human reelin promoter. *Nucleic Acids Res* 2002; **30**: 2930–2939.
6 Abdolmaleky HM, Cheng KH, Russo A, Smith CL, Faraone SV, Wilcox M *et al*. Hypermethylation of the reelin (RELN) promoter in the brain of schizophrenic patients: a preliminary report. *Am J Med Genet B Neuropsychiatr Genet* 2005; **134**: 60–66.
7 Dong E, Agis-Balboa RC, Simonini MV, Grayson DR, Costa E, Guidotti A. Reelin and glutamic acid decarboxylase67 promoter remodeling in an epigenetic methionine-induced mouse model of schizophrenia. *Proc Natl Acad Sci USA* 2005; **102**: 12578–12583.
8 Popendikyte V, Laurinavicius A, Paterson AD, Macciardi F, Kennedy JL, Petronis A. DNA methylation at the putative promoter region of the human dopamine D2 receptor gene. *Neuroreport* 1999; **10**: 1249–1255.
9 Hohjoh H, Singer MF. Cytoplasmic ribonucleoprotein complexes containing human LINE-1 protein and RNA. *Embo J* 1996; **15**: 630–639.
10 Fatemi SH, Earle JA, McMenomy T. Reduction in Reelin immunoreactivity in hippocampus of subjects with schizophrenia, bipolar disorder and major depression. *Mol Psychiatry* 2000; **5**: 654–663, 571.
11 Fatemi SH, Emamian ES, Kist D, Sidwell RW, Nakajima K, Akhter P *et al*. Defective corticogenesis and reduction in Reelin immunoreactivity in cortex and hippocampus of prenatally infected neonatal mice. *Mol Psychiatry* 1999; **4**: 145–154.

12 Impagnatiello F, Guidotti AR, Pesold C, Dwivedi Y, Caruncho H, Pisu MG *et al*. A decrease of reelin expression as a putative vulnerability factor in schizophrenia. *Proc Natl Acad Sci USA* 1998; **95**: 15718–15723.

13 Guidotti A, Auta J, Davis JM, Di-Giorgi-Gerevini V, Dwivedi Y, Grayson DR *et al*. Decrease in reelin and glutamic acid decarboxylase67 (GAD67) expression in schizophrenia and bipolar disorder: a postmortem brain study. *Arch Gen Psychiatry* 2000; **57**: 1061–1069.

14 Eastwood SL, Harrison PJ. Interstitial white matter neurons express less reelin and are abnormally distributed in schizophrenia: towards an integration of molecular and morphologic aspects of the neurodevelopmental hypothesis. *Mol Psychiatry* 2003; **8**: 769, 821–831.

15 Noh JS, Sharma RP, Veldic M, Salvacion AA, Jia X, Chen Y *et al*. DNA methyltransferase 1 regulates reelin mRNA expression in mouse primary cortical cultures. *Proc Natl Acad Sci USA* 2005; **102**: 1749–1754.

16 Ekelund J, Lichtermann D, Hovatta I, Ellonen P, Suvisaari J, Terwilliger JD *et al*. Genome-wide scan for schizophrenia in the Finnish population: evidence for a locus on chromosome 7q22. *Hum Mol Genet* 2000; **9**: 1049–1057.

European Journal of Neuroscience, Vol. 27, pp. 691–701, 2008 doi:10.1111/j.1460-9568.2008.06047.x

Reduction in memory in passive avoidance learning, exploratory behaviour and synaptic plasticity in mice with a spontaneous deletion in the ubiquitin C-terminal hydrolase L1 gene

Mikako Sakurai,[1,*] Masayuki Sekiguchi,[1,2,*] Ko Zushida,[1,2] Kazuyuki Yamada,[3] Satoshi Nagamine,[1] Tomohiro Kabuta[1] and Keiji Wada[1,2]

[1]Department of Degenerative Neurological Diseases, National Institute of Neuroscience, National Center of Neurology and Psychiatry, 4-1-1 Ogawahigashi, Kodaira, Tokyo 187–8502, Japan

[2]CREST, Japan Science and Technology Agency, Kawaguchi, Saitama 322–0012, Japan

[3]Support Unit for Animal Experiments, Brain Science Institute, RIKEN, 2–1 Hirosawa, Wako, Saitama 351–0198, Japan

Keywords: Alzheimer's disease, CREB, hippocampus, LTP, transcription

Abstract

Overexpression of ubiquitin C-terminal hydrolase L1 (UCH-L1) in mice rescues amyloid β-protein-induced decreases in synaptic plasticity and memory. However, the physiological role of UCH-L1 in the brain is not fully understood. In the present study, we investigated the role of UCH-L1 in the brain by utilizing gracile axonal dystrophy (*gad*) mice with a spontaneous deletion in the gene *Uch-l1* as a loss-of-function model. Although *gad* mice exhibit motor paresis beginning at ~12 weeks of age, it is possible to analyse their brain phenotypes at a younger age when no motor paresis is evident. Maintenance of memory in a passive avoidance test and exploratory behaviour in an open field test were reduced in 6-week-old *gad* mice. The maintenance of theta-burst stimulation-induced long-term potentiation (LTP) of field synaptic responses from Schaffer collaterals to CA1 pyramidal cells in hippocampal slices was also impaired in *gad* mice. The LTP in *gad* mice was insensitive to actinomycin D, suggesting that a transcription-dependent component of the LTP is impaired. Phosphorylation of cyclic AMP response element binding protein (CREB) in the CA1 region of hippocampal slices from *gad* mice occurred earlier than in the slices from wild-type mice and was transient, suggesting that CREB phosphorylation is altered in *gad* mice. These results suggest that memory in passive avoidance learning, exploratory behaviour and hippocampal CA1 LTP are reduced in *gad* mice. We propose that UCH-L1-mediated maintenance of the temporal integrity and persistence of CREB phosphorylation underlies these impairments.

Introduction

Ubiquitin C-terminal hydrolase L1 (UCH-L1) is a deubiquitinating enzyme (Wilkinson *et al.*, 1989) that is exclusively expressed in the brain and testis, and its expression is neuron-specific in the brain (Wilkinson *et al.*, 1989). Several lines of evidence suggest that UCH-L1 is involved in idiopathic Alzheimer's disease (AD) and Parkinson's disease (PD): (i) UCH-L1 is down-regulated in idiopathic AD and PD (Choi *et al.*, 2004), and in an AD model mouse (Gong *et al.*, 2006); and (ii) UCH-L1 is oxidatively modified in AD brains (Castegna *et al.*, 2002). Substitution of tyrosine for serine at codon 18 (S18Y polymorphism) in the *Uch-l1* gene exerts a protective effect against sporadic AD (Xue & Jia, 2006) and PD (Maraganore *et al.*, 1999). Furthermore, substitution of methionine for isoleucine at codon 93 (I93M mutation) reduces hydrolase activity of UCH-L1 and is linked to a rare autosomal dominant form of familial PD in a German family (Leroy *et al.*, 1998). Although these findings point to a role for UCH-L1 in AD and PD, the physiological role of UCH-L1 in the normal mammalian brain is not fully understood.

UCH-L1 has multiple functions *in vitro*. UCH-L1 removes small adducts or unfolded polypeptides from ubiquitin's C-terminus via hydrolysis (Larsen *et al.*, 1998). In addition, UCH-L1 has ubiquitin-ligase activity on α-synuclein-ubiquitin conjugates (Liu *et al.*, 2002). Apart from enzymatic activity, UCH-L1 acts as a stabilizer of monoubiquitin (Osaka *et al.*, 2003). UCH-L1 is thought to be a therapeutic target for AD; specifically, overexpression of UCH-L1 rescues amyloid β-protein (Aβ)-induced decreases in synaptic plasticity and contextual memory in mice (Gong *et al.*, 2006). Pharmacological suppression of UCH-L1 hydrolase activity (by 70%) is associated with impairment of synaptic transmission, tetanus-induced long-term potentiation (LTP) in the hippocampal CA1 field, and contextual fear memory in mice (Gong *et al.*, 2006). The nonmammalian Aplysia UCH has been identified as an immediate–early gene essential for long-term synaptic facilitation in the nervous system (Hedge *et al.*, 1997).

The aim of the present study was to further characterize the role of UCH-L1 in the mammalian brain. To this end, we utilized the UCH-L1-deficient *gracile axonal dystrophy* (*gad*) mouse, which is a spontaneous mutant with an in-frame deletion in exons 7 and 8 of *Uch-l1* (Saigoh *et al.*, 1999). Expression of the UCH-L1 protein is

Correspondence: Dr Keiji Wada, [1]Department of Degenerative Neurological Diseases, as above.
E-mail: wada@ncnp.go.jp

*M. Sakurai and M. Sekiguchi contributed equally to this study

Received 12 July 2007, revised 10 December 2007, accepted 12 December 2007

undetectable in the central nervous system of *gad* mice (Osaka *et al.*, 2003). In addition, recent analysis in our laboratory suggests that truncated products from the mutant *Uch-l1* are not detected in the *gad* mouse brain (T. Kabuta, unpublished observation). Although *gad* mice exhibit motor paresis beginning at ~12 weeks of age due to axonal degeneration of spinal cord neurons and subsequent degeneration of the spinocerebellar tract (Kikuchi *et al.*, 1990), it is possible to analyse the brain phenotypes of *gad* mice at younger ages when no motor paresis is evident. We found that memory in passive avoidance learning, exploratory behaviour and hippocampal synaptic plasticity are reduced in young *gad* mice (6 weeks of age).

Materials and Methods

Animals

Gad mice were bred at the Experimental Animal Center of the National Institute of Neuroscience, National Center of Neurology and Psychiatry, Tokyo. The original genetic background of *gad* mice was a hybrid of the CBA and RFM strains (Kikuchi *et al.*, 1990). However, *gad* mice were backcrossed to C57BL/6J strain mice 6–18 times before use in the present study. Six-week-old male *gad* mice and wild-type mice generated from heterozygous *gad* mating pairs were used for the experiments. Genotyping was carried out using PCR with the following three primers:

F1, 5′- agcttggagcctgtggtttcaactc-3′;
R1, 5′-tggcagcatcctgaaaaggagaggtg-3′;
R2, 5′-tacagatggccgtccacgttgttga-3′

The reaction conditions were 35 cycles of 94 °C for 20 s, 60 °C for 30 s and 72 °C for 60 s. The wild-type allele produced an 891-bp PCR product, and the *gad* allele produced a 446-bp PCR product. Three to five mice were housed per cage under controlled temperature (25 ± 1 °C) and lighting (12-h light–dark cycle) conditions and provided with food and water *ad libitum*. The experiments were performed in strict accordance with the National Institute of Neuroscience's regulations for animal experimentation, and were approved by the Animal Investigation Committee of the Institute.

Histology

Hematoxylin and eosin (H&E) staining was performed as reported (Kikuchi *et al.*, 1990). For immunohistochemistry, 4-μm-thick paraffin sections were de-paraffinized and pretreated in a microwave oven with 10 mM citrate–NaOH buffer (pH 6.0). After blocking with phosphate-buffered saline containing 1% heat-inactivated normal goat serum and 0.1% [(v/v)] Triton X-100, slides were incubated with an anti-Aβ monoclonal antibody (clone 4G8, 1 : 100 dilution; Signet Laboratories, Dedham, MA, USA) or an antisynaptophysin monoclonal antibody (MAB5258, 1 : 500 dilution; Chemicon, Temecula, CA, USA) and then with Envision+horseradish peroxidase–labelled anti-mouse IgG (DakoCytomation Inc., Carpinteria, CA, USA). Chromogenic detection was performed using the DAB Substrate kit (DakoCytomation Inc.). Sections were examined with a BX51 microscope (Olympus).

Behavioural tests

One-trial passive avoidance tests were performed as described (Yamada *et al.*, 2003). Briefly, a single mouse was introduced into a light compartment of a light–dark box (Muromachi-kikai, Tokyo, Japan). During habituation, mice were allowed to freely explore the box for 5 min with the sliding door between the light and dark compartments open; after that, the mice were returned to their home cage. For conditioning, which was carried out 2 h after habituation, the mice were introduced into the light compartment, the sliding door was closed when both hindlimbs had entered into the dark box, and an electrical footshock was delivered via the floor grid in the dark compartment (300 μA, 3 s duration, using a shock generator–scrambler; Muromachi-kikai). The mice were left in the light–dark box for 5 min and then returned to their home cage. Tests were carried out 2 or 24 h after the conditioning by re-introducing the mice into the light compartment of the light–dark box. The latency time for mice to enter the dark compartment was measured (light–dark latency, with a 5 min cut-off). The tests at 2 and 24 h postconditioning were carried out using different groups of mice.

The pain sensitivity of mice was tested as described (Yamada *et al.*, 2003). Briefly, a series of footshocks of ascending (20, 40, 60, 80, 100 and 130 μA, 1 s duration) and descending (130, 100, 80, 60, 40 and 20 μA, 1 s duration) current were serially delivered to the mice via the floor grid. The input current that induced hindlimb withdraw was recorded. The interfootshock interval was 15 s. This trial was performed six times, and the data were averaged.

Open field tests were performed as we described (Zushida *et al.*, 2007). Briefly, the test was carried out in an arena (a 50 × 50 cm white field surrounded by a 40-cm-high white wall, illuminated with 80 lx) placed in a soundproof box. Mice were placed at the periphery of the arena, and for 5 min the behaviour of the mice was recorded using a digital video camera linked to a computer. Locomotor activity was calculated from this record by Image OF (O'Hara & Co., Ltd, Tokyo, Japan), modified software based on the public domain NIH Image program. Rearing was manually counted.

The light–dark box test was performed as described (Yamada *et al.*, 2002). Briefly, mice were placed into the dark compartment of the light–dark box and were allowed to explore both sides of the light–dark box for 5 min. During these 5 min, three parameters were measured: latency to enter the light compartment, number of entries into the light compartment, and duration in the light compartment.

Electrophysiology

Each 6-week-old male mouse was anaesthetized with halothane, and the brain was quickly removed. Preparation of hippocampal slices for electrophysiology was carried out as reported (Takamatsu *et al.*, 2005; Zushida *et al.*, 2007). Briefly, the hippocampus was isolated from the brain, and transverse slices (400 μm thick) were prepared using a Vibratome 3000 microtome (Vibratome Company, St Louis, MO, USA) in a sucrose-based cutting solution (in mM: sucrose, 234; KCl, 25; NaH_2PO_4, 1.25; $MgSO_4$, 10; $NaHCO_3$, 26; glucose, 11; and $CaCl_2$, 0.5). The slices were maintained at room temperature in artificial cerebrospinal fluid (ACSF; in mM: NaCl, 125; KCl, 4.4; $MgSO_4$, 1.5; NaH_2PO_4, 1.0; $NaHCO_3$, 26; glucose, 10; and $CaCl_2$, 2.5; pH 7.4, 290–300 mOsm/L) continuously bubbled with 95% O_2 and 5% CO_2. A slice was then transferred to the recording chamber and was continuously superfused at 3 mL/min with ACSF maintained at 28–32 °C.

Extracellular field recordings were carried out as reported (Takamatsu *et al.*, 2005). Briefly, field excitatory postsynaptic potentials (fEPSPs) were recorded from CA1 stratum radiatum of the hippocampus using a glass micropipette (1–2 MΩ) filled with ACSF. The electrical signals were amplified using a MultiClamp 700B amplifier (Axon Instruments, Foster City, CA, USA), filtered at 10 kHz, digitized at 10 kHz and acquired with Clampex (ver. 9.2). A bipolar stainless steel stimulating electrode was placed in stratum radiatum at the border between CA2 and CA3 to stimulate the Schaffer collateral pathway. The pulse intensity was adjusted to give 40% of the maximum amplitude in all experiments. Stimulation was carried out in

constant current mode (100 μs duration). The fEPSPs for which the 40% amplitude was > 1 mV were used for data analysis. The strength of synaptic transmission was determined by measuring the rising phase (20–60%) of the fEPSP slope. The average fEPSP slope during the 10 min prior to LTP induction was taken as the baseline, and all values were normalized to this baseline. The baseline stimulation frequency was 0.033 Hz. LTP was induced by applying theta-burst stimulation (TBS; 15 bursts of four pulses at 100 Hz, delivered at an interburst interval of 200 ms) or tetanic stimulation (100 Hz, 1 s, three times with a 20 s interval). Paired-pulse facilitation was induced by delivering two consecutive pulses with a 20-, 50-, 100-, 200- or 400-ms interpulse interval.

Somatic whole-cell patch-clamp recordings were made with a MultiClamp 700B amplifier (Zushida *et al.*, 2007). Pyramidal-shaped neurons in the CA1 pyramidal layer visually identified with differential contrast video microscopy (Hamamatsu Photonics, Hamamatsu, Japan) on an upright microscope (Axioscope, Zeiss, Oberkochen, Germany) were selected for recording. The patch electrodes were 6–10 MΩ when filled with a solution containing (in mM): K gluconate, 132; KCl, 3; HEPES, 10; EGTA, 0.5; $MgCl_2$, 1; sodium phosphocreatine, 12; ATP·Mg, 3; and GTP, 0.5 (pH 7.4 with KOH, 285–290 mOsm/L). We used this solution when measuring membrane potential and input resistance. The input resistance was calculated by injecting a square current pulse (−10 pA) in current-clamp mode. For comparison of synaptic currents at −70 and +40 mV, an internal solution containing (in mM): CsOH, 105; CsCl, 30; HEPES, 10; EGTA, 0.5; $MgCl_2$, 1; sodium phosphocreatine, 12; ATP·Mg, 3; and GTP, 0.5 (pH 7.3 with gluconic acid, 295 mOsm/L) was used. The signal was digitized at one point per 50 μs and stored using Clampex. The resting membrane potential of the cells used in the analysis ranged from −57 to −67 mV, and the series resistance was 3–20 MΩ. Synaptic responses were elicited by electrical stimulation as described for extracellular recording. The pulse intensity was adjusted to elicit excitatory postsynaptic potentials (EPSPs) 40% of the amplitude required for action potential generation in current-clamp mode.

All chemicals and drugs used for electrophysiology were purchased from Sigma with the exception of actinomycin D, which was obtained from Wako Pure Chemicals (Tokyo, Japan). Actinomycin D was dissolved in dimethylsulfoxide at 40 mM, added to ACSF just prior to application at 40 μM, and bath-applied with perfusion. Therefore, the final dimethylsulfoxide concentration was 0.1%.

Western blotting

For analysis of Aβ, the hippocampus was isolated from the brain and snap-frozen in liquid nitrogen. The tissue was homogenized in ice-cold buffer (Tris-HCl, 50 mM; NaCl, 150 mM; EDTA, 5 mM; and Triton X-100, 1%; pH 7.5) containing proteinase inhibitors (Complete, EDTA-free; Roche Applied Science, Indianapolis, IN, USA) and phosphatase inhibitors (Halt phosphatase inhibitor cocktail; Pierce, Rockford, IL, USA), and the homogenate was subjected to SDS-PAGE. Western blotting was carried out as we reported (Kabuta *et al.*, 2006) using anti-Aβ (clone 4G8; Signet Laboratories), anti-UCH-L1 (UltraClone Ltd, UK) and anti-β-actin (Sigma) antibodies. Briefly, immunoreactive signals were visualized with SuperSignal West Femto maximum sensitivity substrate (Pierce) or SuperSignal West Dura extended duration substrate (Pierce) and detected with a chemiluminescence imaging system (FluorChem; Alpha Innotech, San Leandro, CA, USA). Human Aβ 1–42 from Peptide Institute, Inc., Osaka, Japan served as the positive control.

Following extracellular recording, hippocampal slices were retrieved for Western blotting. The dentate gyrus and CA3 region of the slices were cut off, and the remaining CA1 region was snap-frozen in liquid nitrogen. Tissue samples from each slice were homogenized in the same buffer as used for the Aβ analysis, and the homogenate was subjected to SDS-PAGE. The antibodies used were anti-phospho-CREB (serine 133), anti-CREB (Cell Signalling Technology, Inc., Danvers, MA, USA), anti-cAMP-dependent protein kinase (protein kinase A; PKA) regulatory subunit RIα and RIIα (BD Biosciences, San Jose, CA, USA), anti-UCH-L1 (UltraClone Ltd) and anti-β-actin (Sigma). Immunoreactive signals were visualized as described for the Aβ analysis. The signal intensity was quantified by densitometry using FluoChem software (Alpha Innotech).

Data and statistical analysis

Numerical data are expressed as the mean ± SEM. The two-tailed Student's *t*-test was used for comparison between wild-type mice and *gad* mice. Repeated-measures one-way ANOVA was used to analyse whether footshock and exposure to an open field arena had significant effects within a genotype in passive avoidance and open field tests, respectively. ANOVA with the Bonferroni–Dunn test was used to compare the three data groups in the pCREB analysis.

Results

Structural abnormalities were not detected in the cerebrum and hippocampus of young gad mice

Before behavioural analysis, we first examined whether there were any histological abnormalities in the cerebral cortex and hippocampus of 6-week-old *gad* mice. It has been reported that the thalamus is not impaired in *gad* mice (Kikuchi *et al.*, 1990), but there is no report on the cortex and limbic system. Figure 1A–D shows H&E staining of coronal brain sections (at bregma level −1.7 mm) from a wild-type mouse (Fig. 1A and C) and *gad* mouse (Fig. 1B and D; 6 weeks of age). We could not detect any visible abnormalities, such as atrophy or lack of cells, in the hippocampus or cortex of *gad* mice ($n = 2$). One anatomical characteristic of *gad* mice is spheroid structures in the medulla and spinal cord that are thought to be degenerating axons (Kikuchi *et al.*, 1990). We did not find this aberration in the hippocampus or cortex of *gad* mice (Fig. 1A–D). We also examined other brain regions in sections cut at bregma levels 2.5, 1.0, −3.0 and −6.0 mm, and no outstanding abnormalities were evident in the *gad* mice (data not shown). In addition, we carried out immunohistochemical staining using antisynaptophysin. This antibody stains presynaptic sites and thus the staining pattern would be expected to be different in *gad* mice if there was noticeable axonal degeneration. Typical punctate synaptophysin staining was obtained in both wild-type (Fig. 1E and G) and *gad* (Fig. 1F and H) mice. We could not detect any visible differences in the staining of the hippocampus between wild-type and *gad* mice. These results suggest that structural impairment of the brain at a macroanatomical level is not evident in 6-week-old *gad* mice.

Axonal degeneration promotes accumulation of Aβ in the medulla and spinal cord of *gad* mice (Ichihara *et al.*, 1995). Consistent with the lack of spheroid structures in the cortex and hippocampus, we did not find abnormal accumulation of Aβ in these brain regions in *gad* mice up to 12 weeks of age (immunohistochemical analysis using an antibody to Aβ; data not shown). Furthermore, we examined nonfibrillar Aβ by Western blotting. We could not detect any significant bands in the samples from wild-type and *gad* mouse hippocampi when blotting with anti-Aβ (Fig. 1I, upper panel). Authentic human Aβ (the right two lanes, a positive control) blotted

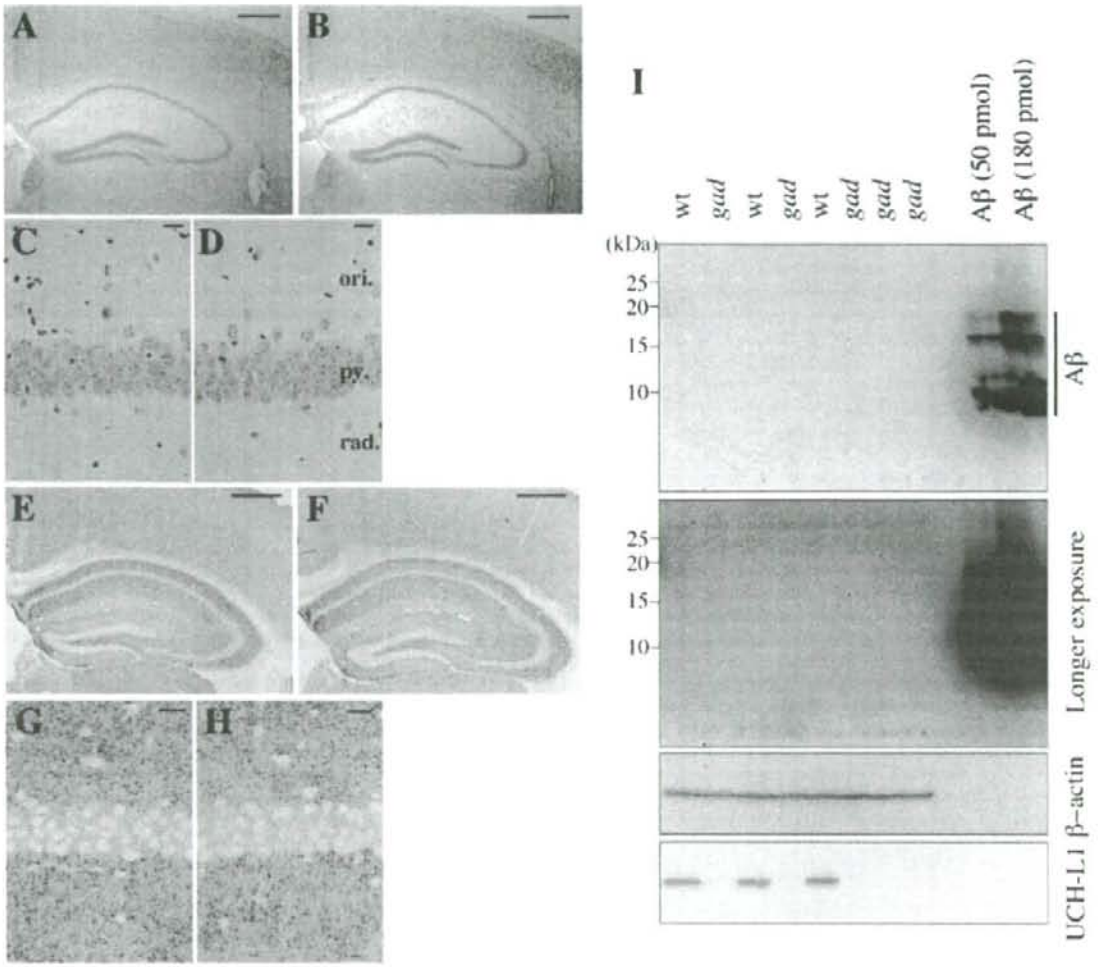

FIG. 1. Six-week-old *gad* mice have normal brain histology. (A–D) H&E staining of coronal brain sections from (A and C) a 6-week-old wild-type (wt) mouse and (B and D) a 6-week-old *gad* mouse. (C and D) A higher magnification of the hippocampal CA1 field. ori., stratum oriens; py., pyramidal cell layer; rad., stratum radiatum. (E–H) Synaptophysin immunohistochemistry in coronal brain sections from a six-week-old wt mouse (E and G) and a six-week-old *gad* mouse (F and H). (G and H) A higher magnification of the hippocampal CA1 field. (I) Western blotting of samples prepared from the hippocampi of three wt and five *gad* mice. Antibodies against Aβ, β-actin and UCH-L1 were used. Authentic Aβ was used as a positive control. A short exposure is shown in the upper panel; a longer exposure is shown below. Molecular size markers (kDa) are shown on the left. Scale bars, 500 μm (A, B, E and F), 20 μm (C, D, G and H).

densely on the same membrane. After a longer exposure (Fig. 1I) we could detect certain bands, but there was no band that was significantly increased in *gad* mice compared with wild-type mice. Blots using antiβ-actin and anti-UCH-L1 were carried out to confirm the sample load and genotype, respectively (Fig. 1I).

Lack of UCH-L1 in mice impaired memory maintenance in the passive avoidance test and exploratory behaviour for a novel environment

Next, we examined whether lack of UCH-L1 had a detectable impact on mouse behaviour. For this purpose, we carried out one-trial passive avoidance tests. Figure 2A shows the performance of wild-type and *gad* mice in this test. After habituation to the light–dark box, mice were conditioned with an electrical footshock when they entered the dark compartment. We then tested their ability to avoid the dark compartment 24 h after the conditioning footshock. The footshock significantly prolonged the light–dark latency in wild-type mice (comparison of the conditioning and test sessions $P = 0.003$, $F = 14.6$, $n = 12$; repeated-measures ANOVA). In contrast, the light–dark latency was not significantly affected in *gad* mice (comparison of the conditioning and test sessions using repeated-measures ANOVA, $P = 0.2437$, $F = 1.556$, $n = 10$), suggesting that memory function, as assessed by this test, is impaired in *gad* mice. In

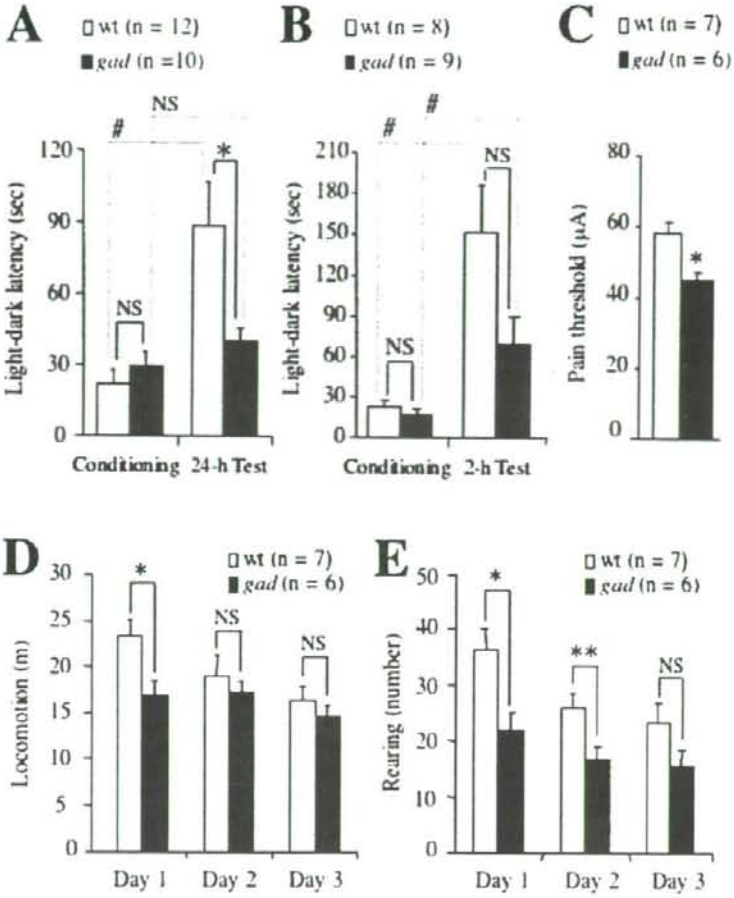

FIG. 2. Impairment of memory maintenance and exploratory behaviour in *gad* mice. (A and B) Light–dark latency of mice in a one-trial passive avoidance test. After habituation to a light–dark box, mice were conditioned with an electrical footshock when they entered the dark compartment (Conditioning). At (A) 24 h or (B) 2 h after the footshock, the mice were reintroduced into the light–dark box and the time for mice to enter the dark compartment (light–dark latency) was measured (Test). $^{*}P = 0.028$; NS, not significant; two-tailed Student's *t*-test (solid lines). $^{\#}P < 0.020$; NS, not significant, repeated-measures one-way ANOVA (dotted lines). (C) Pain sensitivity of the mice was measured by applying a series of electrical footshocks. $^{*}P = 0.002$, two-tailed Student's *t*-test. (D) Locomotor activity of wild-type and *gad* mice in an open field arena. The mice were introduced into the arena for the first time on day 1. $^{*}P = 0.023$, two-tailed Student's *t*-test. (E) Rearing frequency of wild-type and *gad* mice in an open field arena. $^{*}P = 0.014$, $^{**}P = 0.021$; two-tailed Student's *t*-test.

addition, the light–dark latency in the 24-h test session differed significantly between the wild-type and *gad* mice ($P = 0.028$; two-tailed Student's *t*-test). We next conducted a test session 2 h after conditioning to test whether learning ability was impaired in *gad* mice shortly after conditioning. In the test 2 h after conditioning (Fig. 2B), the footshock had a significant effect on the light–dark latency in both wild-type and *gad* mice ($P = 0.0147$, $F = 10.356$, $n = 8$ for wild-type mice; $P = 0.0199$, $F = 8.407$, $n = 9$ for *gad* mice; repeated-measures ANOVA). The average latency in the 2-h test session did not differ significantly between the wild-type and *gad* mice ($P = 0.074$; two-tailed Student's *t*-test). These results suggest that *gad* mice are able to learn but maintenance of memory is reduced. Because the pain sensitivity of *gad* mice was greater than that of wild-type mice (Fig. 2C; $P = 0.002$ with two-tailed Student's *t*-test), the footshock used for conditioning was indeed an aversive stimulus in *gad* mice.

Next, we carried out the open field test. Mice were exposed to an open field arena for the first time on day 1 (Fig. 2D). The wild-type mice explored the novel environment and showed high locomotor activity (Fig. 2D). Locomotor activity was reduced upon re-exposure of wild-type mice to the same arena on days 2 and 3 because they remembered the arena, and thus the novelty was reduced ($P = 0.024$, $F = 12.928$, $n = 7$; repeated-measures ANOVA). In contrast, locomotor activity was not significantly decreased in *gad* mice ($P = 0.392$, $F = 1.030$, $n = 6$; repeated-measures ANOVA). The locomotor activity on day 1 differed significantly between wild-type and *gad* mice ($P = 0.023$; two-tailed Student's *t*-test), but the activity on day 2 or 3 did not ($P = 0.500$ and 0.446 for days 2 and

3, respectively). To determine whether the difference in locomotor activity on day 1 was due to reduced exploratory behaviour in *gad* mice, we measured the frequency of rearing, a typical exploratory behaviour (Lever *et al.*, 2006; Fig. 2E). Similar to locomotor activity, upon re-exposure rearing frequency decreased in wild-type mice ($P = 0.009$, $F = 14.257$, $n = 7$; repeated-measures ANOVA) but not in *gad* mice ($P = 0.131$, $F = 2.503$, $n = 6$; repeated-measures ANOVA). The rearing frequency on days 1 and 2 differed significantly between wild-type and *gad* mice ($P = 0.014$ and 0.021 for days 1 and 2, respectively; two-tailed Student's *t*-test), but the activity on day 3 did not ($P = 0.093$). These results suggest that exploratory behaviour in a novel environment is reduced in *gad* mice.

Although these data apparently suggest that memory in passive avoidance learning and exploratory behaviour are reduced in young *gad* mice, there is a possibility that the anxiety state of *gad* mice is altered. Alterations in the anxiety state can affect memory (Bouton *et al.*, 1990) and the response to novel environments. To measure anxiety, we performed a light–dark box test. In this test, mice usually avoid the light compartment. Therefore, the level of anxiety can be measured as the latency to move into the light compartment and the duration of time in the light compartment (Yamada *et al.*, 2002). Because the passive avoidance test also utilizes these properties, performance in the light–dark test is important for interpreting the results from the passive avoidance test. The time required for the mice to step into the light compartment when introduced into the dark compartment (dark-light latency; Fig. 3A), the time the mice spent in the light compartment (Fig. 3A) and the number of times the mice crossed between compartments (Fig. 3B) did not differ significantly between wild-type and *gad* mice ($P = 0.834$, 0.417 and 0.109, respectively; two-tailed Student's *t*-test). These results suggest that anxiety state, as assessed by this test, was not obviously altered in *gad* mice. Therefore we concluded that the impairments in passive avoidance learning and exploratory behaviour were not due to alterations in the anxiety state.

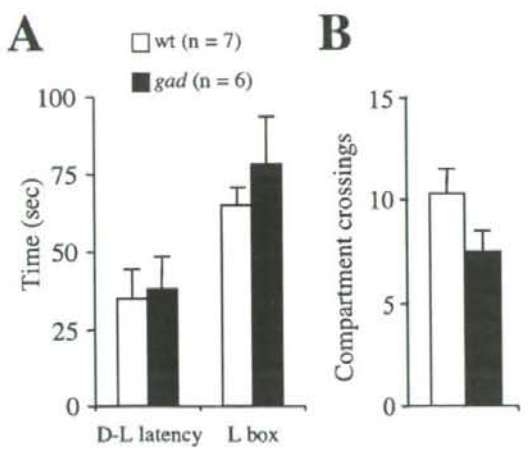

FIG. 3. Wild-type and *gad* mice performed similarly in the light–dark box test. (A) Dark–light (D-L) latency and duration of time in the light compartment (L box). (B) Number of crossings between the two compartments.

Impairment of a transcription-dependent component of LTP in gad mice

We tested whether the lack of UCH-L1 affects neuronal function by measuring LTP at Schaffer collateral synapses onto CA1 pyramidal neurons in hippocampal slice preparations. LTP is believed to be a synaptic mechanism underlying memory and learning (Bliss & Collingridge, 1993). The CA1 synapse was selected because this brain region is involved in spatial memory (Morris *et al.*, 1982) and passive avoidance memory (Bevilaqua *et al.*, 1997; Impey *et al.*, 1998). In wild-type slices, TBS induced robust LTP at CA1 synapses (Fig. 4A), as reported for C57BL/6J mice (Nguyen & Kandel, 1997; Nguyen *et al.*, 2000). In contrast, TBS-induced LTP was attenuated in *gad* mice beginning ~20 min post-TBS (Fig. 4A). At 45 min post-TBS, normalized synaptic responses were significantly greater in wild-type slices (1.87 ± 0.08, $n = 7$) than in *gad* slices (1.36 ± 0.07, $n = 6$; $P = 0.001$, two-tailed Student's *t*-test). Impairment of LTP in *gad* mice depended on the stimulation pattern. Tetanus-induced LTP was identical in wild-type and *gad* mice (Fig. 4B; normalized fEPSP slopes at 45 min post-tetanus: wild-type, 1.81 ± 0.16, $n = 5$; *gad*, 1.86 ± 0.25, $n = 5$).

Stimulus–output curves (Fig. 5A) and paired-pulse facilitation (Fig. 5B) of CA1 synapses were essentially identical in wild-type and *gad* mice. The latter result suggests that a postsynaptic, rather than presynaptic, mechanism is involved in impairment of TBS-induced LTP in *gad* mice. LTP at this synapse is dependent on postsynaptic NMDA receptors (Harris *et al.*, 1984; Larson & Lynch, 1988). Therefore, we tested whether NMDA receptor activity was reduced in *gad* mice using patch-clamp recordings. For this purpose, we recorded Schaffer collateral–CA1 synaptic responses in neurons voltage-clamped to −70 and +40 mV in the presence of picrotoxin (50 μM). The amplitude of the synaptic response recorded at +40 mV at 100 ms poststimulation was normalized to the peak amplitude of the response at −70 mV to estimate the ratio of NMDA-mediated to non-NMDA-mediated currents (Fig. 5D). Because superfusion of the slices with picrotoxin frequently elicited epileptiform activity (data not shown), three to five synaptic responses without epileptiform activity were selected and averaged. The ratio was identical in wild-type and *gad* mice (0.45 ± 0.05, $n = 5$ and 0.43 ± 0.05, $n = 7$ for wild-type and *gad* mice, respectively; two-tailed Student's *t*-test). Therefore, attenuation of synaptic NMDA receptor activity does not account for reduced LTP in *gad* mice. Resting membrane potential and input resistance of CA1 pyramidal neurons did not differ substantially between wild-type and *gad* mice [resting membrane potential, -60.1 ± 0.4 mV for wild-type mice ($n = 20$) and -60.0 ± 0.6 mV for *gad* mice ($n = 20$); input resistance, 163 ± 9.6 for wild-type mice ($n = 16$) and 175 ± 10.8 for *gad* mice ($n = 13$); results obtained from the records using potassium-gluconate pipette solution].

CA1 LTP is composed of early and late temporal phases (Nguyen *et al.*, 1994; Abel *et al.*, 1997; Nguyen & Kandel, 1997). The former is induced mainly by an increase in the number of AMPA-type glutamate receptors at the synapse (reviewed in Malinow & Malenka, 2002) whereas the latter is induced by new protein synthesis from transcription of new mRNA (Nguyen *et al.*, 1994) and/or local protein synthesis from previously expressed mRNA (Bradshaw *et al.*, 2003). Because no obvious changes in the early phase of LTP (up to ~20 min post-TBS) were observed in *gad* mice, we tested whether the late phase is occluded in *gad* mice. For this purpose, we applied actinomycin D, a transcription inhibitor, to the slices and compared suppression of TBS-induced LTP in wild-type and *gad* mice. In wild-type mice, the maintenance of TBS-induced LTP was suppressed by actinomycin D (Fig. 6A). The normalized fEPSP slope at 45 min

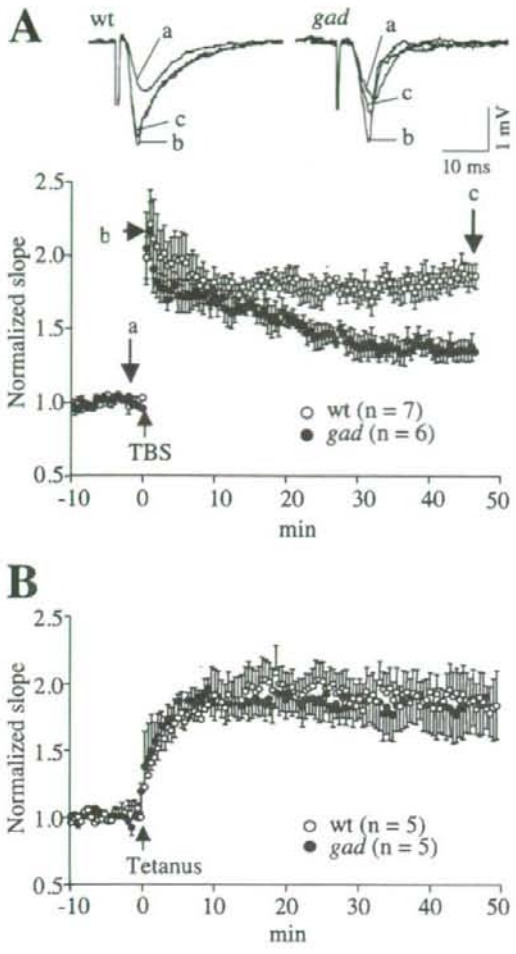

FIG. 4. TBS-induced LTP in area CA1 of the *gad* mouse hippocampus was impaired. (A) LTP induced by TBS in wild-type (○) and *gad* (●) mice. The fEPSP slope was normalized to baseline (pre-TBS) values. Typical fEPSP traces are shown above. Traces were recorded (a) just before TBS, (b) immediately after TBS and (c) 45 min after TBS. (B) Tetanus-induced LTP was identical in wild-type and *gad* mice.

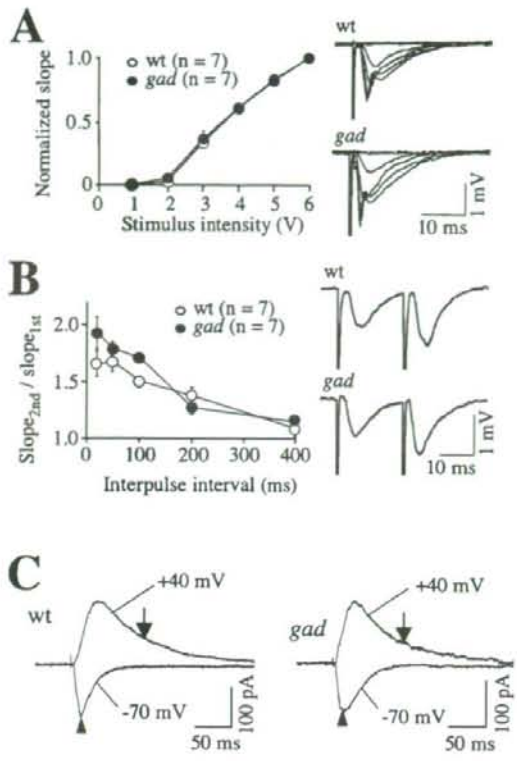

FIG. 5. Stimulus–output curves, paired-pulse facilitation and NMDA receptor-mediated currents were similar in wild-type and *gad* mice. (A) The relation between stimulus intensity and the slope of the fEPSP was identical in wild-type and *gad* mice. For each slice, fEPSP slopes elicited by six different stimulus intensities (1–6 V; sample traces in the right panel) were normalized to the value obtained using 6-V stimulation, and then normalized values were averaged. (B) Paired-pulse facilitation of fEPSPs did not differ substantially between wild-type and *gad* mice. (C) The ratio of NMDA receptor-mediated currents to non-NMDA receptor-mediated currents was identical in wild-type and *gad* mice. Patch-clamp recordings from neurons voltage-clamped to −70 and +40 mV. The arrowhead indicates the peak of the non-NMDA receptor-mediated current, and the arrow indicates 100 ms poststimulation for the NMDA receptor-mediated current; current amplitudes at these points were used for the ratio.

post-TBS was 1.43 ± 0.07 (n = 5) in the presence of actinomycin D, and this value differed significantly from that in wild-type hippocampal slices without actinomycin D (1.87 ± 0.08, P = 0.003; two-tailed Student's t-test). This result agrees with a previous report (Nguyen & Kandel, 1997). In contrast, TBS-induced LTP in *gad* mice was insensitive to actinomycin D (Fig. 6B). The normalized fEPSP slope at 45 min post-TBS was 1.36 ± 0.04 (n = 5) in the presence of actinomycin D and did not differ significantly from the value in *gad* hippocampal slices without actinomycin D (1.36 ± 0.07, P = 0.948; two-tailed Student's t-test). These results suggest that a transcription-dependent component of LTP is impaired in *gad* mice. In both wild-type and *gad* mice, actinomycin D did not affect the baseline fEPSP slope (without TBS) up to 80 min postapplication (Fig. 6C and D).

CREB phosphorylation was altered in gad mice

Late-phase LTP in the hippocampal CA1 field requires transcription elicited by phosphorylation of serine 133 on cAMP response element binding protein (CREB; Nguyen *et al.*, 1994). In addition, Aplysia UCH is involved in persistent activation of PKA during long-term synaptic facilitation (Hedge *et al.*, 1997). From these reports and our experiments using actinomycin D above, we suspected that phosphorylated CREB (pCREB)-induced transcription is disrupted in *gad* mice. To address this, we analysed pCREB in the CA1 field of slices used

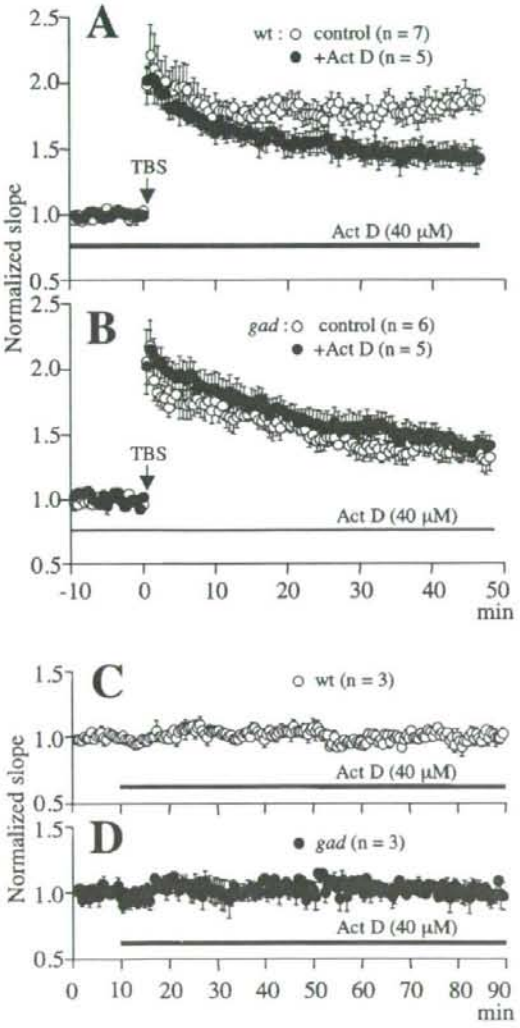

FIG. 6. Transcription-dependent LTP was impaired in *gad* mice. (A and B) Actinomycin D (Act D) suppressed late-phase LTP in (A) wild-type mice but (B) had no effect in *gad* mice. Act D was applied 10 min before LTP induction and was continuously applied until 50 min post-TBS. LTP in the absence of Act D (control) has been reproduced from Fig. 4. (C and D) Without TBS, Act D had no effect on the normalized fEPSP slope in either (C) wild-type or (D) *gad* mice.

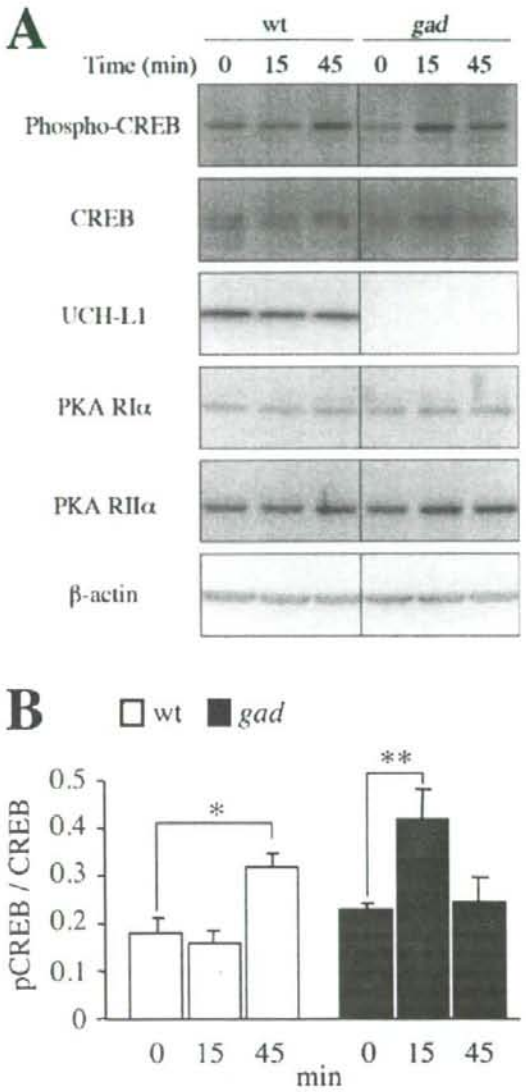

FIG. 7. CREB phosphorylation was altered in *gad* mice. (A) Western blotting of samples prepared from hippocampal slices recovered pre-TBS (0), 15 min post-TBS (15) or 45 min post-TBS (45). Primary antibodies are indicated to the left of the blots. Similar results were obtained at each time point in six slices from wild-type mice and five slices from *gad* mice. (B) The normalized band density of pCREB to CREB at time 0 (pre-TBS), 15 min and 45 min post-TBS in wild-type ($n = 5$) and *gad* ($n = 4$) mice. *$P = 0.012$ and **$P = 0.014$, Bonferroni–Dunn test.

for electrophysiological recording by Western blotting (Fig. 7A). In wild-type mice, pCREB levels at 15 min post-TBS did not differ from pre-TBS levels, but at 45 min post-TBS levels were increased relative to pre-TBS levels. The onset of CREB phosphorylation (45 min postconditioning) is in agreement with a previous report (Ahmed & Frey, 2005). In *gad* mice, however, pCREB levels were increased at 15 min post-TBS but not maintained at 45 min post-TBS (Fig. 7A). Unphosphorylated CREB levels were similar among samples (Fig. 7A). Similar results were obtained in slices from five wild-type and four *gad* mice. In each set of slices, the band density of pCREB was normalized to that of CREB and the values were averaged (Fig. 7B). In wild-type mice (Fig. 7B), the normalized pCREB levels at 15 min post-TBS did not differ significantly from pre-TBS levels